

Evidence for the $\eta_b(1S)$ Meson in Radiative $\Upsilon(2S)$ Decay

B. Aubert,¹ M. Bona,¹ Y. Karyotakis,¹ J. P. Lees,¹ V. Poireau,¹ E. Prencipe,¹ X. Prudent,¹ V. Tisserand,¹ J. Garra Tico,² E. Grauges,² L. Lopez,^{3a,3b} A. Palano,^{3a,3b} M. Pappagallo,^{3a,3b} G. Eigen,⁴ B. Stugu,⁴ L. Sun,⁴ M. Battaglia,⁵ D. N. Brown,⁵ L. T. Kerth,⁵ Yu. G. Kolomensky,⁵ G. Lynch,⁵ I. L. Osipenkov,⁵ K. Tackmann,⁵ T. Tanabe,⁵ C. M. Hawkes,⁶ N. Soni,⁶ A. T. Watson,⁶ H. Koch,⁷ T. Schroeder,⁷ D. J. Asgeirsson,⁸ B. G. Fulsom,⁸ C. Hearty,⁸ T. S. Mattison,⁸ J. A. McKenna,⁸ M. Barrett,⁹ A. Khan,⁹ A. Randle-Conde,⁹ V. E. Blinov,¹⁰ A. D. Bukin,¹⁰ A. R. Buzykaev,¹⁰ V. P. Druzhinin,¹⁰ V. B. Golubev,¹⁰ A. P. Onuchin,¹⁰ S. I. Serednyakov,¹⁰ Yu. I. Skovpen,¹⁰ E. P. Solodov,¹⁰ K. Yu. Todyshev,¹⁰ M. Bondioli,¹¹ S. Curry,¹¹ I. Eschrich,¹¹ D. Kirkby,¹¹ A. J. Lankford,¹¹ P. Lund,¹¹ M. Mandelkern,¹¹ E. C. Martin,¹¹ D. P. Stoker,¹¹ S. Abachi,¹² C. Buchanan,¹² H. Atmacan,¹³ J. W. Gary,¹³ F. Liu,¹³ O. Long,¹³ G. M. Vitug,¹³ Z. Yasin,¹³ L. Zhang,¹³ V. Sharma,¹⁴ C. Campagnari,¹⁵ T. M. Hong,¹⁵ D. Kovalskyi,¹⁵ M. A. Mazur,¹⁵ J. D. Richman,¹⁵ T. W. Beck,¹⁶ A. M. Eisner,¹⁶ C. A. Heusch,¹⁶ J. Kroseberg,¹⁶ W. S. Lockman,¹⁶ A. J. Martinez,¹⁶ T. Schalk,¹⁶ B. A. Schumm,¹⁶ A. Seiden,¹⁶ L. O. Winstrom,¹⁶ C. H. Cheng,¹⁷ D. A. Doll,¹⁷ B. Echenard,¹⁷ F. Fang,¹⁷ D. G. Hitlin,¹⁷ I. Narsky,¹⁷ T. Piatenko,¹⁷ F. C. Porter,¹⁷ R. Andreassen,¹⁸ G. Mancinelli,¹⁸ B. T. Meadows,¹⁸ K. Mishra,¹⁸ M. D. Sokoloff,¹⁸ P. C. Bloom,¹⁹ W. T. Ford,¹⁹ A. Gaz,¹⁹ J. F. Hirschauer,¹⁹ M. Nagel,¹⁹ U. Nauenberg,¹⁹ J. G. Smith,¹⁹ S. R. Wagner,¹⁹ R. Ayad,^{20,*} A. Soffer,^{20,†} W. H. Toki,²⁰ R. J. Wilson,²⁰ E. Feltresi,²¹ A. Hauke,²¹ H. Jasper,²¹ M. Karbach,²¹ J. Merkel,²¹ A. Petzold,²¹ B. Spaan,²¹ K. Wacker,²¹ M. J. Kobel,²² R. Nogowski,²² K. R. Schubert,²² R. Schwierz,²² A. Volk,²² D. Bernard,²³ G. R. Bonneaud,²³ E. Latour,²³ M. Verderi,²³ P. J. Clark,²⁴ S. Playfer,²⁴ J. E. Watson,²⁴ M. Andreotti,^{25a,25b} D. Bettoni,^{25a} C. Bozzi,^{25a} R. Calabrese,^{25a,25b} A. Cecchi,^{25a,25b} G. Cibinetto,^{25a,25b} P. Franchini,^{25a,25b} E. Luppi,^{25a,25b} M. Negrini,^{25a,25b} A. Petrella,^{25a,25b} L. Piemontese,^{25a} V. Santoro,^{25a,25b} R. Baldini-Ferroli,²⁶ A. Calcaterra,²⁶ R. de Sangro,²⁶ G. Finocchiaro,²⁶ S. Pacetti,²⁶ P. Patteri,²⁶ I. M. Peruzzi,^{26,‡} M. Piccolo,²⁶ M. Rama,²⁶ A. Zallo,²⁶ R. Contri,^{27a,27b} M. Lo Vetere,^{27a,27b} M. R. Monge,^{27a,27b} S. Passaggio,^{27a} C. Patrignani,^{27a,27b} E. Robutti,^{27a} S. Tosi,^{27a,27b} K. S. Chaisanguanthum,²⁸ M. Morii,²⁸ A. Adametz,²⁹ J. Marks,²⁹ S. Schenk,²⁹ U. Uwer,²⁹ F. U. Bernlochner,³⁰ V. Klose,³⁰ H. M. Lacker,³⁰ D. J. Bard,³¹ P. D. Dauncey,³¹ M. Tibbetts,³¹ P. K. Behera,³² X. Chai,³² M. J. Charles,³² U. Mallik,³² J. Cochran,³³ H. B. Crawley,³³ L. Dong,³³ W. T. Meyer,³³ S. Prell,³³ E. I. Rosenberg,³³ A. E. Rubin,³³ Y. Y. Gao,³⁴ A. V. Gritsan,³⁴ Z. J. Guo,³⁴ N. Arnaud,³⁵ J. Béquilleux,³⁵ A. D'Orazio,³⁵ M. Davier,³⁵ J. Firmino da Costa,³⁵ G. Grosdidier,³⁵ F. Le Diberder,³⁵ V. Lepeltier,³⁵ A. M. Lutz,³⁵ S. Pruvot,³⁵ P. Roudeau,³⁵ M. H. Schune,³⁵ J. Serrano,³⁵ V. Sordini,^{35,§} A. Stocchi,³⁵ G. Wormser,³⁵ D. J. Lange,³⁶ D. M. Wright,³⁶ I. Bingham,³⁷ J. P. Burke,³⁷ C. A. Chavez,³⁷ J. R. Fry,³⁷ E. Gabathuler,³⁷ R. Gamet,³⁷ D. E. Hutchcroft,³⁷ D. J. Payne,³⁷ C. Touramanis,³⁷ A. J. Bevan,³⁸ C. K. Clarke,³⁸ F. Di Lodovico,³⁸ R. Sacco,³⁸ M. Sigamani,³⁸ G. Cowan,³⁹ S. Paramesvaran,³⁹ A. C. Wren,³⁹ D. N. Brown,⁴⁰ C. L. Davis,⁴⁰ A. G. Denig,⁴¹ M. Fritsch,⁴¹ W. Gradl,⁴¹ K. E. Alwyn,⁴² D. Bailey,⁴² R. J. Barlow,⁴² G. Jackson,⁴² G. D. Lafferty,⁴² T. J. West,⁴² J. I. Yi,⁴² J. Anderson,⁴³ C. Chen,⁴³ A. Jawahery,⁴³ D. A. Roberts,⁴³ G. Simi,⁴³ J. M. Tuggle,⁴³ C. Dallapiccola,⁴⁴ E. Salvati,⁴⁴ S. Saremi,⁴⁴ R. Cowan,⁴⁵ D. Dujmic,⁴⁵ P. H. Fisher,⁴⁵ S. W. Henderson,⁴⁵ G. Sciolla,⁴⁵ M. Spitznagel,⁴⁵ F. Taylor,⁴⁵ R. K. Yamamoto,⁴⁵ M. Zhao,⁴⁵ P. M. Patel,⁴⁶ S. H. Robertson,⁴⁶ A. Lazzaro,^{47a,47b} V. Lombardo,^{47a} F. Palombo,^{47a,47b} J. M. Bauer,⁴⁸ L. Cremaldi,⁴⁸ R. Godang,^{48,||} R. Kroeger,⁴⁸ D. J. Summers,⁴⁸ H. W. Zhao,⁴⁸ M. Simard,⁴⁹ P. Taras,⁴⁹ H. Nicholson,⁵⁰ G. De Nardo,^{51a,51b} L. Lista,^{51a} D. Monorchio,^{51a,51b} G. Onorato,^{51a,51b} C. Sciacca,^{51a,51b} G. Raven,⁵² H. L. Snoek,⁵² C. P. Jessop,⁵³ K. J. Knoepfel,⁵³ J. M. LoSecco,⁵³ W. F. Wang,⁵³ L. A. Corwin,⁵⁴ K. Honscheid,⁵⁴ H. Kagan,⁵⁴ R. Kass,⁵⁴ J. P. Morris,⁵⁴ A. M. Rahimi,⁵⁴ J. J. Regensburger,⁵⁴ S. J. Sekula,⁵⁴ Q. K. Wong,⁵⁴ N. L. Blount,⁵⁵ J. Brau,⁵⁵ R. Frey,⁵⁵ O. Igonkina,⁵⁵ J. A. Kolb,⁵⁵ M. Lu,⁵⁵ R. Rahmat,⁵⁵ N. B. Sinev,⁵⁵ D. Strom,⁵⁵ J. Strube,⁵⁵ E. Torrence,⁵⁵ G. Castelli,^{56a,56b} N. Gagliardi,^{56a,56b} M. Margoni,^{56a,56b} M. Morandin,^{56a} M. Posocco,^{56a} M. Rotondo,^{56a} F. Simonetto,^{56a,56b} R. Stroili,^{56a,56b} C. Voci,^{56a,56b} P. del Amo Sanchez,⁵⁷ E. Ben-Haim,⁵⁷ H. Briand,⁵⁷ J. Chauveau,⁵⁷ O. Hamon,⁵⁷ Ph. Leruste,⁵⁷ J. Ocariz,⁵⁷ A. Perez,⁵⁷ J. Prendki,⁵⁷ S. Sitt,⁵⁷ L. Gladney,⁵⁸ M. Biasini,^{59a,59b} E. Manoni,^{59a,59b} C. Angelini,^{60a,60b} G. Batignani,^{60a,60b} S. Bettarini,^{60a,60b} G. Calderini,^{60a,60b,¶} M. Carpinelli,^{60a,60b,**} A. Cervelli,^{60a,60b} F. Forti,^{60a,60b} M. A. Giorgi,^{60a,60b} A. Lusiani,^{60a,60c} G. Marchiori,^{60a,60b} M. Morganti,^{60a,60b} N. Neri,^{60a,60b} E. Paoloni,^{60a,60b} G. Rizzo,^{60a,60b} J. J. Walsh,^{60a} D. Lopes Pegna,⁶¹ C. Lu,⁶¹ J. Olsen,⁶¹ A. J. S. Smith,⁶¹ A. V. Telnov,⁶¹ F. Anulli,^{62a} E. Baracchini,^{62a,62b} G. Cavoto,^{62a} R. Faccini,^{62a,62b} F. Ferrarotto,^{62a} F. Ferroni,^{62a,62b} M. Gaspero,^{62a,62b} P. D. Jackson,^{62a} L. Li Gioi,^{62a} M. A. Mazzoni,^{62a} S. Morganti,^{62a} G. Piredda,^{62a} F. Renga,^{62a,62b} C. Voena,^{62a} M. Ebert,⁶³ T. Hartmann,⁶³ H. Schröder,⁶³ R. Waldi,⁶³ T. Adye,⁶⁴ B. Franek,⁶⁴ E. O. Olaiya,⁶⁴ F. F. Wilson,⁶⁴ S. Emery,⁶⁵ L. Esteve,⁶⁵ G. Hamel de Monchenault,⁶⁵ W. Kozanecki,⁶⁵ G. Vasseur,⁶⁵ Ch. Yèche,⁶⁵ M. Zito,⁶⁵ X. R. Chen,⁶⁶ H. Liu,⁶⁶ W. Park,⁶⁶ M. V. Purohit,⁶⁶ R. M. White,⁶⁶ J. R. Wilson,⁶⁶ M. T. Allen,⁶⁷

D. Aston,⁶⁷ R. Bartoldus,⁶⁷ J. F. Benitez,⁶⁷ R. Cenci,⁶⁷ J. P. Coleman,⁶⁷ M. R. Convery,⁶⁷ J. C. Dingfelder,⁶⁷ J. Dorfan,⁶⁷ G. P. Dubois-Felsmann,⁶⁷ W. Dunwoodie,⁶⁷ R. C. Field,⁶⁷ A. M. Gabareen,⁶⁷ M. T. Graham,⁶⁷ P. Grenier,⁶⁷ C. Hast,⁶⁷ W. R. Innes,⁶⁷ J. Kaminski,⁶⁷ M. H. Kelsey,⁶⁷ H. Kim,⁶⁷ P. Kim,⁶⁷ M. L. Kocian,⁶⁷ D. W. G. S. Leith,⁶⁷ S. Li,⁶⁷ B. Lindquist,⁶⁷ S. Luitz,⁶⁷ V. Luth,⁶⁷ H. L. Lynch,⁶⁷ D. B. MacFarlane,⁶⁷ H. Marsiske,⁶⁷ R. Messner,⁶⁷ D. R. Muller,⁶⁷ H. Neal,⁶⁷ S. Nelson,⁶⁷ C. P. O'Grady,⁶⁷ I. Ofte,⁶⁷ M. Perl,⁶⁷ B. N. Ratcliff,⁶⁷ A. Roodman,⁶⁷ A. A. Salnikov,⁶⁷ R. H. Schindler,⁶⁷ J. Schwiening,⁶⁷ A. Snyder,⁶⁷ D. Su,⁶⁷ M. K. Sullivan,⁶⁷ K. Suzuki,⁶⁷ S. K. Swain,⁶⁷ J. M. Thompson,⁶⁷ J. Va'vra,⁶⁷ A. P. Wagner,⁶⁷ M. Weaver,⁶⁷ C. A. West,⁶⁷ W. J. Wisniewski,⁶⁷ M. Wittgen,⁶⁷ D. H. Wright,⁶⁷ H. W. Wulsin,⁶⁷ A. K. Yarritu,⁶⁷ K. Yi,⁶⁷ C. C. Young,⁶⁷ V. Ziegler,⁶⁷ P. R. Burchat,⁶⁸ A. J. Edwards,⁶⁸ T. S. Miyashita,⁶⁸ S. Ahmed,⁶⁹ M. S. Alam,⁶⁹ J. A. Ernst,⁶⁹ B. Pan,⁶⁹ M. A. Saeed,⁶⁹ S. B. Zain,⁶⁹ S. M. Spanier,⁷⁰ B. J. Wogland,⁷⁰ R. Eckmann,⁷¹ J. L. Ritchie,⁷¹ A. M. Ruland,⁷¹ C. J. Schilling,⁷¹ R. F. Schwitters,⁷¹ B. W. Drummond,⁷² J. M. Izen,⁷² X. C. Lou,⁷² F. Bianchi,^{73a,73b} D. Gamba,^{73a,73b} M. Pelliccioni,^{73a,73b} M. Bomben,^{74a,74b} L. Bosisio,^{74a,74b} C. Cartaro,^{74a,74b} G. Della Ricca,^{74a,74b} L. Lanceri,^{74a,74b} L. Vitale,^{74a,74b} V. Azzolini,⁷⁵ N. Lopez-March,⁷⁵ F. Martinez-Vidal,⁷⁵ D. A. Milanes,⁷⁵ A. Oyangueren,⁷⁵ J. Albert,⁷⁶ Sw. Banerjee,⁷⁶ B. Bhuyan,⁷⁶ H. H. F. Choi,⁷⁶ K. Hamano,⁷⁶ G. J. King,⁷⁶ R. Kowalewski,⁷⁶ M. J. Lewczuk,⁷⁶ I. M. Nugent,⁷⁶ J. M. Roney,⁷⁶ R. J. Sobie,⁷⁶ T. J. Gershon,⁷⁷ P. F. Harrison,⁷⁷ J. Ilic,⁷⁷ T. E. Latham,⁷⁷ G. B. Mohanty,⁷⁷ E. M. T. Puccio,⁷⁷ H. R. Band,⁷⁸ X. Chen,⁷⁸ S. Dasu,⁷⁸ K. T. Flood,⁷⁸ Y. Pan,⁷⁸ R. Prepost,⁷⁸ C. O. Vuosalo,⁷⁸ and S. L. Wu⁷⁸

(BABAR Collaboration)

¹Laboratoire de Physique des Particules, IN2P3/CNRS et Université de Savoie, F-74941 Annecy-Le-Vieux, France

²Universitat de Barcelona, Facultat de Física, Departament ECM, E-08028 Barcelona, Spain

^{3a}INFN Sezione di Bari, I-70126 Bari, Italy

^{3b}Dipartimento di Fisica, Università di Bari, I-70126 Bari, Italy

⁴University of Bergen, Institute of Physics, N-5007 Bergen, Norway

⁵Lawrence Berkeley National Laboratory and University of California, Berkeley, California 94720, USA

⁶University of Birmingham, Birmingham, B15 2TT, United Kingdom

⁷Ruhr Universität Bochum, Institut für Experimentalphysik 1, D-44780 Bochum, Germany

⁸University of British Columbia, Vancouver, British Columbia, Canada V6T 1Z1

⁹Brunel University, Uxbridge, Middlesex UB8 3PH, United Kingdom

¹⁰Budker Institute of Nuclear Physics, Novosibirsk 630090, Russia

¹¹University of California at Irvine, Irvine, California 92697, USA

¹²University of California at Los Angeles, Los Angeles, California 90024, USA

¹³University of California at Riverside, Riverside, California 92521, USA

¹⁴University of California at San Diego, La Jolla, California 92093, USA

¹⁵University of California at Santa Barbara, Santa Barbara, California 93106, USA

¹⁶University of California at Santa Cruz, Institute for Particle Physics, Santa Cruz, California 95064, USA

¹⁷California Institute of Technology, Pasadena, California 91125, USA

¹⁸University of Cincinnati, Cincinnati, Ohio 45221, USA

¹⁹University of Colorado, Boulder, Colorado 80309, USA

²⁰Colorado State University, Fort Collins, Colorado 80523, USA

²¹Technische Universität Dortmund, Fakultät Physik, D-44221 Dortmund, Germany

²²Technische Universität Dresden, Institut für Kern- und Teilchenphysik, D-01062 Dresden, Germany

²³Laboratoire Leprince-Ringuet, CNRS/IN2P3, Ecole Polytechnique, F-91128 Palaiseau, France

²⁴University of Edinburgh, Edinburgh EH9 3JZ, United Kingdom

^{25a}INFN Sezione di Ferrara, I-44100 Ferrara, Italy

^{25b}Dipartimento di Fisica, Università di Ferrara, I-44100 Ferrara, Italy

²⁶INFN Laboratori Nazionali di Frascati, I-00044 Frascati, Italy

^{27a}INFN Sezione di Genova, I-16146 Genova, Italy

^{27b}Dipartimento di Fisica, Università di Genova, I-16146 Genova, Italy

²⁸Harvard University, Cambridge, Massachusetts 02138, USA

²⁹Universität Heidelberg, Physikalisches Institut, Philosophenweg 12, D-69120 Heidelberg, Germany

³⁰Humboldt-Universität zu Berlin, Institut für Physik, Newtonstr. 15, D-12489 Berlin, Germany

³¹Imperial College London, London, SW7 2AZ, United Kingdom

³²University of Iowa, Iowa City, Iowa 52242, USA

³³Iowa State University, Ames, Iowa 50011-3160, USA

³⁴Johns Hopkins University, Baltimore, Maryland 21218, USA

- ³⁵Laboratoire de l'Accélérateur Linéaire, IN2P3/CNRS et Université Paris-Sud 11, Centre Scientifique d'Orsay, B. P. 34, F-91898 Orsay Cedex, France
- ³⁶Lawrence Livermore National Laboratory, Livermore, California 94550, USA
- ³⁷University of Liverpool, Liverpool L69 7ZE, United Kingdom
- ³⁸Queen Mary, University of London, London, E1 4NS, United Kingdom
- ³⁹University of London, Royal Holloway and Bedford New College, Egham, Surrey TW20 0EX, United Kingdom
- ⁴⁰University of Louisville, Louisville, Kentucky 40292, USA
- ⁴¹Johannes Gutenberg-Universität Mainz, Institut für Kernphysik, D-55099 Mainz, Germany
- ⁴²University of Manchester, Manchester M13 9PL, United Kingdom
- ⁴³University of Maryland, College Park, Maryland 20742, USA
- ⁴⁴University of Massachusetts, Amherst, Massachusetts 01003, USA
- ⁴⁵Massachusetts Institute of Technology, Laboratory for Nuclear Science, Cambridge, Massachusetts 02139, USA
- ⁴⁶McGill University, Montréal, Québec, Canada H3A 2T8
- ^{47a}INFN Sezione di Milano, I-20133 Milano, Italy
- ^{47b}Dipartimento di Fisica, Università di Milano, I-20133 Milano, Italy
- ⁴⁸University of Mississippi, University, Mississippi 38677, USA
- ⁴⁹Université de Montréal, Physique des Particules, Montréal, Québec, Canada H3C 3J7
- ⁵⁰Mount Holyoke College, South Hadley, Massachusetts 01075, USA
- ^{51a}INFN Sezione di Napoli, I-80126 Napoli, Italy
- ^{51b}Dipartimento di Scienze Fisiche, Università di Napoli Federico II, I-80126 Napoli, Italy
- ⁵²NIKHEF, National Institute for Nuclear Physics and High Energy Physics, NL-1009 DB Amsterdam, The Netherlands
- ⁵³University of Notre Dame, Notre Dame, Indiana 46556, USA
- ⁵⁴Ohio State University, Columbus, Ohio 43210, USA
- ⁵⁵University of Oregon, Eugene, Oregon 97403, USA
- ^{56a}INFN Sezione di Padova, I-35131 Padova, Italy
- ^{56b}Dipartimento di Fisica, Università di Padova, I-35131 Padova, Italy
- ⁵⁷Laboratoire de Physique Nucléaire et de Hautes Energies, IN2P3/CNRS, Université Pierre et Marie Curie-Paris6, Université Denis Diderot-Paris7, F-75252 Paris, France
- ⁵⁸University of Pennsylvania, Philadelphia, Pennsylvania 19104, USA
- ^{59a}INFN Sezione di Perugia, I-06100 Perugia, Italy
- ^{59b}Dipartimento di Fisica, Università di Perugia, I-06100 Perugia, Italy
- ^{60a}INFN Sezione di Pisa, I-56127 Pisa, Italy
- ^{60b}Dipartimento di Fisica, Università di Pisa, I-56127 Pisa, Italy
- ^{60c}Scuola Normale Superiore di Pisa, I-56127 Pisa, Italy
- ⁶¹Princeton University, Princeton, New Jersey 08544, USA
- ^{62a}INFN Sezione di Roma, I-00185 Roma, Italy
- ^{62b}Dipartimento di Fisica, Università di Roma La Sapienza, I-00185 Roma, Italy
- ⁶³Universität Rostock, D-18051 Rostock, Germany
- ⁶⁴Rutherford Appleton Laboratory, Chilton, Didcot, Oxon, OX11 0QX, United Kingdom
- ⁶⁵CEA, Irfu, SPP, Centre de Saclay, F-91191 Gif-sur-Yvette, France
- ⁶⁶University of South Carolina, Columbia, South Carolina 29208, USA
- ⁶⁷SLAC National Accelerator Laboratory, Stanford, California 94309, USA
- ⁶⁸Stanford University, Stanford, California 94305-4060, USA
- ⁶⁹State University of New York, Albany, New York 12222, USA
- ⁷⁰University of Tennessee, Knoxville, Tennessee 37996, USA
- ⁷¹University of Texas at Austin, Austin, Texas 78712, USA
- ⁷²University of Texas at Dallas, Richardson, Texas 75083, USA
- ^{73a}INFN Sezione di Torino, I-10125 Torino, Italy
- ^{73b}Dipartimento di Fisica Sperimentale, Università di Torino, I-10125 Torino, Italy
- ^{74a}INFN Sezione di Trieste, I-34127 Trieste, Italy
- ^{74b}Dipartimento di Fisica, Università di Trieste, I-34127 Trieste, Italy
- ⁷⁵IFIC, Universitat de Valencia-CSIC, E-46071 Valencia, Spain
- ⁷⁶University of Victoria, Victoria, British Columbia, Canada V8W 3P6
- ⁷⁷Department of Physics, University of Warwick, Coventry CV4 7AL, United Kingdom
- ⁷⁸University of Wisconsin, Madison, Wisconsin 53706, USA

(Received 6 March 2009; published 15 October 2009)

We have performed a search for the $\eta_b(1S)$ meson in the radiative decay of the $\Upsilon(2S)$ resonance using a sample of 91.6×10^6 $\Upsilon(2S)$ events recorded with the BABAR detector at the PEP-II B factory at the SLAC National Accelerator Laboratory. We observe a peak in the photon energy spectrum at $E_\gamma = 609.3_{-4.5}^{+4.6}(\text{stat}) \pm 1.9(\text{syst})$ MeV, corresponding to an $\eta_b(1S)$ mass of $9394.2_{-4.9}^{+4.8}(\text{stat}) \pm 2.0(\text{syst})$ MeV/ c^2 .

The branching fraction for the decay $Y(2S) \rightarrow \gamma\eta_b(1S)$ is determined to be $[3.9 \pm 1.1(\text{stat})_{-0.9}^{+1.1}(\text{syst})] \times 10^{-4}$. We find the ratio of branching fractions $\mathcal{B}[Y(2S) \rightarrow \gamma\eta_b(1S)]/\mathcal{B}[Y(3S) \rightarrow \gamma\eta_b(1S)] = 0.82 \pm 0.24(\text{stat})_{-0.19}^{+0.20}(\text{syst})$.

DOI: 10.1103/PhysRevLett.103.161801

PACS numbers: 13.20.Gd, 14.40.Gx, 14.65.Fy

A candidate for the $\eta_b(1S)$ meson, the ground state of the bottomonium system, was recently observed in the radiative decays of the $Y(3S)$ [1]. The *BABAR* experiment has accumulated a large sample of data at the peak of the $Y(2S)$ resonance, where radiative $Y(2S)$ decays are also expected to produce the $\eta_b(1S)$ meson. Theoretical predictions for $\mathcal{B}[Y(2S) \rightarrow \gamma\eta_b(1S)]$ range from $(1-15) \times 10^{-4}$ [2]. A 90% confidence level upper limit of $\mathcal{B}[Y(2S) \rightarrow \gamma\eta_b(1S)] < 5.1 \times 10^{-4}$ is provided by the CLEO III experiment [3].

The ratio of branching fractions for the transitions $Y(2S) \rightarrow \gamma\eta_b(1S)$ and $Y(3S) \rightarrow \gamma\eta_b(1S)$ is dependent upon the overlap integrals of the relevant bottomonium wave functions [2], enabling a test that the observed state is the $\eta_b(1S)$ meson. More generally, the measured hyperfine mass splitting between the triplet and singlet states in the bottomonium system provides a better understanding of nonrelativistic bound states in QCD and the role of spin-spin interactions in quarkonium models [4,5].

In this Letter, we report evidence for the radiative transition $Y(2S) \rightarrow \gamma\eta_b(1S)$. Hereafter $\eta_b(1S)$ will be abbreviated as η_b .

The data used in this analysis were collected with the *BABAR* detector [6] at the PEP-II asymmetric-energy e^+e^- storage rings. The primary data sample consists of 14 fb^{-1} of integrated luminosity collected at the peak of the $Y(2S)$ resonance. An additional sample of 44 fb^{-1} collected 40 MeV below the $Y(4S)$ resonance is used for background and efficiency studies. The trajectories of charged particles are reconstructed with a combination of five layers of double-sided silicon strip detectors and a 40-layer drift chamber, both operated in the 1.5-T magnetic field of a superconducting solenoid. Photons are detected with a CsI(Tl) electromagnetic calorimeter (EMC). The photon energy resolution varies from 3.4% (at 300 MeV) to 2.8% (at 800 MeV). Hereafter we quote values of E_γ measured in the center-of-mass (c.m.) frame.

The signal for $Y(2S) \rightarrow \gamma\eta_b$ is extracted from a fit to the inclusive photon energy spectrum. The monochromatic photon from this decay should appear as a peak in the photon energy spectrum near 615 MeV on top of a smooth nonpeaking background from continuum ($e^+e^- \rightarrow q\bar{q}$ with $q = u, d, s, c$) events and bottomonium decays.

Two other processes produce peaks in the photon energy spectrum close to the signal region: ISR production of the $Y(1S)$ and double radiative decays of the $Y(2S)$. The second transition in the processes $Y(2S) \rightarrow \gamma\chi_{bJ}(1P)$, $\chi_{bJ}(1P) \rightarrow \gamma Y(1S)$, $J = 0, 1, 2$, produces peaks centered at 391, 423, and 442 MeV, respectively. These three peaks

are merged due to photon energy resolution and the small Doppler broadening that arises from the motion of the $\chi_{bJ}(1P)$ in the c.m. frame. We use the $\chi_{bJ}(1P) \rightarrow \gamma Y(1S)$ signal to validate estimates of signal efficiencies and determine the absolute photon energy scale. Radiative production of the $Y(1S)$ via initial state radiation (ISR), $e^+e^- \rightarrow \gamma_{\text{ISR}} Y(1S)$, leads to a peak near 550 MeV. The signal peak is better separated from the peaking background, with respect to the $Y(3S) \rightarrow \gamma\eta_b$ analysis [1], primarily due to better absolute energy resolution at lower energy.

Decays of the η_b via two gluons, expected to be its dominant decay mode, have high charged-particle multiplicity. We select hadronic events by requiring four or more charged tracks in the event and that the ratio of the second to zeroth Fox-Wolfram moments [7] be less than 0.98.

Photon candidates are required to be isolated from all charged tracks. To ensure that their EMC shapes are consistent with an electromagnetic shower, the lateral moment [8] is required to be less than 0.55. To ensure high reconstruction efficiency and good energy resolution, the signal photon candidate is required to lie in the central angular region of the EMC, $-0.762 < \cos(\theta_{\gamma,\text{LAB}}) < 0.890$, where $\theta_{\gamma,\text{LAB}}$ is the angle between the photon and the beam axis in the laboratory frame.

The correlation of the direction of the photon with the thrust axis [9] of the η_b is small, as there is no preferred direction in the decay of the spin-zero η_b and the momentum of the η_b is small in the c.m. frame. In contrast, there is a strong correlation between the photon direction and thrust axis in continuum events. The thrust axis is computed with all charged tracks and neutral calorimeter clusters in the event, with the exception of the signal photon candidate. A requirement of $|\cos\theta_T| < 0.8$ is made to reduce continuum background, where θ_T is the angle between the thrust axis and the momentum of the signal photon candidate.

A principle source of background is photons from π^0 decays. A signal photon candidate is rejected if in combination with another photon in the event it forms a π^0 candidate whose mass is within $15 \text{ MeV}/c^2$ of the nominal π^0 mass. To maintain high signal efficiency, we require the second photon of the π^0 candidate to have an energy in the laboratory frame greater than 40 MeV.

The final efficiency evaluated from simulated events is 35.8%.

The selection criteria were chosen by maximizing the ratio $N_S/\sqrt{N_T}$, where N_S is the signal yield and N_T is the total yield of events in the signal region. The result of the

optimization is insensitive to the exact definition of the signal region. A detailed Monte Carlo (MC) simulation [10] provides the signal sample for this optimization, while a small fraction (7%) of the $Y(2S)$ data is used to model the background. To avoid a potential bias, these data are excluded from the final fit of the photon energy spectrum. The remaining $Y(2S)$ data used for the analysis have an integrated luminosity of 13 fb^{-1} , corresponding to (91.6 ± 0.9) million $Y(2S)$ events.

To extract the η_b signal, a χ^2 fit of the E_γ spectrum is performed in the region $0.27 < E_\gamma < 0.80 \text{ GeV}$. The fit includes four components: nonpeaking background, $\chi_{bJ}(1P) \rightarrow \gamma Y(1S)$, $\gamma_{\text{ISR}} Y(1S)$, and the η_b signal.

The nonpeaking background is parametrized by an empirical probability density function (PDF) $A \exp(\sum_{i=1}^4 c_i x^i)$, where $x = E_\gamma$, and A , c_i are determined in the fit.

Doppler-broadened Crystal Ball (CB) functions [11] are used as phenomenological PDFs for the three $\chi_{bJ}(1P) \rightarrow \gamma Y(1S)$ shapes. The CB function is a Gaussian modified to have an extended power-law tail on the low (left) side. The power-law parameter describing the low-side tail of the CB function is common to all three of the $\chi_{bJ}(1P)$ peaks. The Doppler broadening of the $\chi_{bJ}(1P)$ peaks is modeled by analytically convolving the CB functions with rectangular functions of half-width 6.5, 5.5, and 4.9 MeV for the $J = 0, 1, 2$ states, respectively. These values are evaluated using the $Y(2S)$ and $\chi_{bJ}(1P)$ masses [12]. The resolution parameter of the $\chi_{b0}(1P)$ PDF is fixed to that of the $\chi_{b2}(1P)$. Because of its small yield and its position on the low side of the $\chi_{bJ}(1P)$ peak, the exact width of the $\chi_{b0}(1P)$ is not crucial. The relative rates of the $\chi_{bJ}(1P)$ components are fixed to values determined from a control sample of $Y(2S) \rightarrow \gamma \chi_{bJ}(1P)$, $\chi_{bJ}(1P) \rightarrow \gamma Y(1S)$, $Y(1S) \rightarrow \mu^+ \mu^-$ events, and the relative peak positions from the world-averaged (PDG) values [12], with a photon energy scale offset determined in the fit.

The PDF of the peaking background from ISR $Y(1S)$ production is parametrized as a CB function with parameters determined from simulated events. The ISR peak position is fixed to the value determined by the $Y(1S)$ and $Y(2S)$ masses [12], minus the energy scale offset shared with the $\chi_{bJ}(1P)$ peaks.

The η_b signal PDF is a nonrelativistic Breit-Wigner function convolved with a CB function to account for the experimental E_γ resolution. The CB parameters are determined from signal MC. Theoretical predictions for the η_b width, based on the expected ratio of the two-photon and two-gluon widths, range from 4 to 20 MeV [13]. Since the width of the η_b is not known, we have chosen a nominal value of 10 MeV, as in the $Y(3S)$ analysis.

The free parameters in the fit are the normalizations of all fit components, all of the nonpeaking background PDF parameters, the η_b peak position, the energy scale offset, the $\chi_{b1}(1P)$ and $\chi_{b2}(1P)$ CB resolutions, and the transition

point between the Gaussian and power-law components of the $\chi_{bJ}(1P)$ CB functions.

Figure 1 shows the photon energy spectrum and the fit result before (a) and after (b) subtraction of the nonpeaking background. The χ^2 per degree of freedom from the fit is 115/93. The line shapes of the three peaking components, $\chi_{bJ}(1P)$, ISR $Y(1S)$, and the η_b signal, are clearly visible in the subtracted spectrum. The η_b signal yield is $12\,800 \pm 3500$ events, and the η_b peak energy is $607.9^{+4.6}_{-4.5} \text{ MeV}$. The observed signal width is consistent with being dominated by the resolution of 18 MeV.

The ISR $Y(1S)$ yield can be estimated from data collected below the $Y(4S)$ resonance. After correcting for the luminosity ratio, and the difference in ISR cross section and detection efficiencies at the two energies, we expect $16\,700 \pm 700 \pm 1200$ ISR $Y(1S)$ events in the on-resonance $Y(2S)$ data sample. The consistency of the observed yield of the $Y(1S)$ component, $16\,800^{+4200}_{-4000}$ events, with the expected value provides an important validation of the fitted background rate near the signal region. The yield and peak position of the η_b signal change

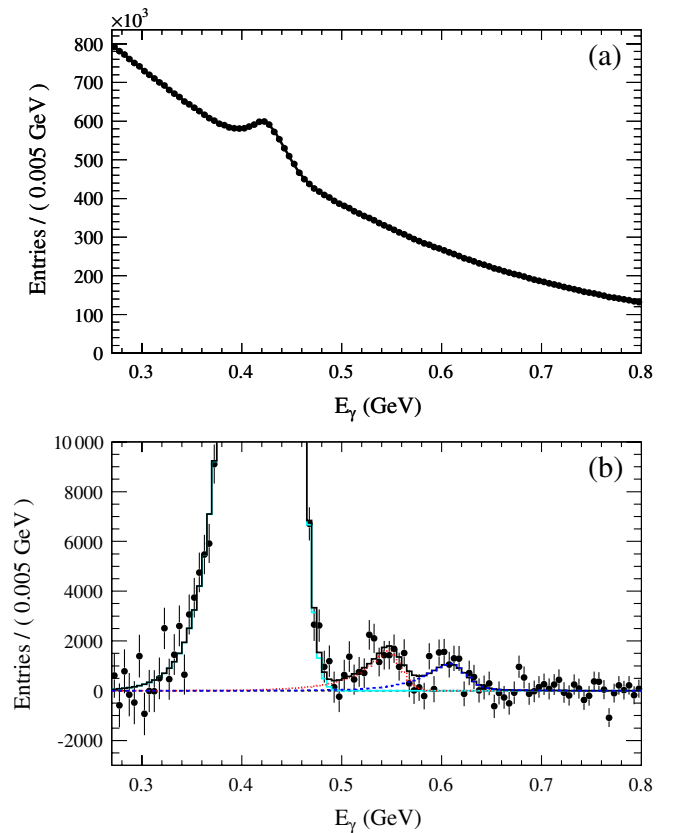


FIG. 1 (color online). (a) Inclusive photon spectrum in the region $0.27 < E_\gamma < 0.80 \text{ GeV}$. The fit is overlaid on the data points. (b) (color online) Inclusive photon spectrum after subtracting the nonpeaking background, with the PDFs for $\chi_{bJ}(1P)$ peak (light solid line), ISR $Y(1S)$ (dotted line), η_b signal (dashed line) and the sum of all three (dark solid line).

by less than 0.1σ when the ISR $Y(1S)$ yield is fixed to the expected value.

We estimate the systematic uncertainty by varying the Breit-Wigner width in the η_b PDF to 5, 15, and 20 MeV, varying the PDF parameters fixed in the fit by $\pm 1\sigma$, using alternative smooth background shapes, varying the histogram binning between 1 and 15 MeV, incorporating a high-side tail to the $\chi_{bJ}(1P)$ peaks, and subtracting possible peaking background components. Smooth background PDF variations consist of using alternative smooth background shapes that either incorporate a 3rd order polynomial in the exponential (i.e., $c_4 = 0$) or use a PDF of the form $k(E_\gamma/E_0)^{-\Gamma_1}[1 + (E_\gamma/E_0)^{1/\alpha}]^{-(\Gamma_2-\Gamma_1)\alpha}$. Other background shape variations consisting of adding a term c_5x^5 to the exponential of the smooth background function or adding a constant background PDF were found to change the fit negligibly. An additional high-side tail in the $\chi_{bJ}(1P)$ peak may be produced by the coincidental overlap of photons from $\chi_{bJ}(1P)$ decays with particles from the rest of the event or beam debris. We model this tail as a 90 MeV wide Gaussian centered about each of the $\chi_{bJ}(1P)$ peaks. Because of the large width of this component, it is indistinguishable from the nonpeaking background, and its inclusion does not improve the fit. We take the difference between the nominal fit and the fit including this tail as a systematic error. To evaluate the systematic due to the $\chi_{b0}(1P)$ resolution, we perform a fit in which the $\chi_{b0}(1P)$ resolution is fixed to that of the $J = 1$ state. To investigate the possible effect of peaking background from $Y(2S) \rightarrow (\pi^0, \eta)Y(1S)$ events, these contributions are subtracted prior to fitting, assuming the measured value and 90% CL upper limits for the branching fraction of the η and π^0 [12] transitions, respectively, giving a variation of $-71 (+651)$ events for the η (π^0) transition. Photons from the transition $Y(2S) \rightarrow \pi^0\pi^0Y(1S)$, which produce a smoothly varying background below 400 MeV, are absorbed into the smooth background PDF and do not require a separate systematic error.

Including systematic uncertainties, the signal yield is $12\,800 \pm 3500_{-3100}^{+3500}$ events. The largest contributions to the systematic error on the η_b yield are from the η_b width variation ($_{-1200}^{+1700}$ events) and the background shape variation ($_{-2700}^{+2600}$ events).

The photon energy scale is corrected with the fitted energy scale offset of $1.4 \pm 0.2 \pm 0.7$ MeV determined from the $\chi_{bJ}(1P)$ and ISR peaks. The systematic error is half of the shift added in quadrature with the PDG errors on the $\chi_{bJ}(1P)$ masses (0.4 MeV). The ISR peak contributes negligibly to the determination of the offset, due to its small yield. After including an additional systematic uncertainty of 1.7 MeV from the fit variations described above, we obtain a value of $E_\gamma = 609.3_{-4.5}^{+4.6} \pm 1.9$ MeV for the η_b signal.

To confirm that this state is identical to the state observed in the $Y(3S) \rightarrow \gamma\eta_b$ analysis [1] we calculate the

significance of the signal with the signal peak fixed to 614.3 MeV, the value expected for an η_b mass of 9388.9 MeV. The η_b signal significance is estimated as $\sqrt{\chi^2(\text{no signal}) - \chi^2(\text{fixed mass})}$, where $\chi^2(\text{fixed mass})$ is the χ^2 of the fit with the η_b signal included and $\chi^2(\text{no signal})$ is the χ^2 of the fit with the η_b PDF removed. The statistical significance estimated in this way is 3.7 standard deviations. The significance of the signal, including systematics, is estimated by making the variations discussed above. Additional cross-checks are performed by changing the lower (upper) limit of the fit range to 250 MeV (850 MeV) and varying the selection on $|\cos(\theta_T)|$. In all fits, the significance lies between 3.0 and 4.3 standard deviations.

The η_b mass derived from the E_γ signal is $M(\eta_b) = 9394.2_{-4.9}^{+4.8} \pm 2.0$ MeV/ c^2 . Using the PDG value of 9460.3 ± 0.3 MeV/ c^2 for the $Y(1S)$ mass, we determine the $Y(1S)$ - η_b mass splitting to be $66.1_{-4.8}^{+4.9} \pm 2.0$ MeV/ c^2 .

For the measurement of the branching fraction, we have an additional source of uncertainty resulting from the signal selection efficiency. The systematic uncertainty on the photon detection efficiency is 1.8%. We estimate the uncertainty on the hadronic selection efficiency (4.9%) by comparing data and MC efficiencies of the selection on hadronic $Y(1S)$ events. The uncertainty in photon quality selection efficiency (0.5%) is estimated from π^0 decays in data and MC. The difference between the efficiency in MC and the efficiency for a flat distribution (0.6%) is used as the uncertainty on the $|\cos\theta_T|$ selection. We determine the uncertainty for the π^0 selection (4.1%) by comparing the efficiency-corrected $\chi_{bJ}(1P)$ yield with and without the π^0 veto. The total systematic error on the selection efficiency is 6.7%. The uncertainty on the number of $Y(2S)$ events is 0.9%. Incorporating these systematic uncertainties, we determine the branching fraction of the decay $Y(2S) \rightarrow \gamma\eta_b$ to be $(3.9 \pm 1.1_{-0.9}^{+1.1}) \times 10^{-4}$.

In the $Y(3S)$ analysis [1], we estimated the systematic uncertainty on the signal efficiency using $\chi_{bJ}(2P)$ decays, incurring a large error (22%) due to the uncertainties in the $\chi_{bJ}(2P)$ branching fractions. The uncertainty in $Y(3S) \rightarrow \gamma\eta_b$ efficiency obtained using the procedure described above is 5.5%, resulting in a final branching fraction of $\mathcal{B}[Y(3S) \rightarrow \gamma\eta_b] = (4.8 \pm 0.5 \pm 0.6) \times 10^{-4}$. This value supersedes our previous result, which differs only in having a systematic uncertainty 2 times larger.

Using the results given above, we determine a branching fraction ratio of $\mathcal{B}[Y(2S) \rightarrow \gamma\eta_b]/\mathcal{B}[Y(3S) \rightarrow \gamma\eta_b] = 0.82 \pm 0.24_{-0.19}^{+0.20}$. The systematic uncertainties due to selection efficiency and the unknown η_b width partially cancel in the ratio. Our measurement is consistent with some of the theoretical estimates of this ratio of magnetic dipole transitions to the η_b , 0.3–0.7 [2], while the absolute transition rates are not well-predicted by theoretical models.

In conclusion, we have obtained evidence, with a significance of 3.0 standard deviations, for the radiative decay

of the $Y(2S)$ to a narrow state with a mass slightly less than that of the $Y(1S)$. The ratio of the radiative production rates for this state at the $Y(2S)$ and $Y(3S)$ resonances is consistent with that expected of the η_b . Under this interpretation, the mass of the η_b is $9394.2^{+4.8}_{-4.9} \pm 2.0 \text{ MeV}/c^2$, which corresponds to a mass splitting between the $Y(1S)$ and the η_b of $66.1^{+4.9}_{-4.8} \pm 2.0 \text{ MeV}/c^2$, consistent with the value from the $Y(3S)$ analysis. The average of the two results is $M(\eta_b) = 9390.8 \pm 3.2 \text{ MeV}/c^2$. This value of the η_b mass is consistent with a recent unquenched lattice prediction [5] but more than 2 standard deviations away from the mass predicted by approaches based on perturbative QCD [14].

We are grateful for the excellent luminosity and machine conditions provided by our PEP-II colleagues, and for the substantial dedicated effort from the computing organizations that support *BABAR*. The collaborating institutions wish to thank SLAC for its support and kind hospitality. This work is supported by DOE and NSF (USA), NSERC (Canada), CEA and CNRS-IN2P3 (France), BMBF and DFG (Germany), INFN (Italy), FOM (The Netherlands), NFR (Norway), MES (Russia), MEC (Spain), and STFC (United Kingdom). Individuals have received support from the Marie Curie EIF (European Union) and the A. P. Sloan Foundation.

*Present address: Temple University, Philadelphia, PA 19122, USA.

†Present address: Tel Aviv University, Tel Aviv, 69978, Israel.

‡Also with Università di Perugia, Dipartimento di Fisica, Perugia, Italy.

§Also with Università di Roma La Sapienza, I-00185 Roma, Italy.

||Present address: University of South Alabama, Mobile, AL 36688, USA.

¶Also with Laboratoire de Physique Nucléaire et de Hautes Energies, IN2P3/CNRS, Université Pierre et Marie Curie-

Paris6, Université Denis Diderot-Paris7, F-75252 Paris, France.

**Also with Università di Sassari, Sassari, Italy.

- [1] B. Aubert *et al.* (*BABAR* Collaboration), Phys. Rev. Lett. **101**, 071801 (2008); **102**, 029901(E) (2009).
- [2] S. Godfrey and J.L. Rosner, Phys. Rev. D **64**, 074011 (2001); **65**, 039901(E) (2002), and references therein.
- [3] M. Artuso *et al.* (CLEO III Collaboration), Phys. Rev. Lett. **94**, 032001 (2005).
- [4] For a comprehensive review, see N. Brambilla *et al.* (Quarkonium Working Group), CERN Yellow Report No. CERN-2005-005, 2005.
- [5] A. Gray *et al.* (HPQCD and UKQCD Collaborations), Phys. Rev. D **72**, 094507 (2005); T. Burch and C. Ehmann, Nucl. Phys. **A797**, 33 (2007); T.-W. Chiu *et al.* (TWQCD Collaboration), Phys. Lett. B **651**, 171 (2007).
- [6] B. Aubert *et al.* (*BABAR* Collaboration), Nucl. Instrum. Methods Phys. Res., Sect. A **479**, 1 (2002).
- [7] G.C. Fox and S. Wolfram, Nucl. Phys. **B149**, 413 (1979).
- [8] A. Drescher *et al.* (ARGUS Collaboration), Nucl. Instrum. Methods Phys. Res., Sect. A **237**, 464 (1985).
- [9] S. Brandt *et al.*, Phys. Lett. **12**, 57 (1964); E. Farhi, Phys. Rev. Lett. **39**, 1587 (1977).
- [10] The *BABAR* detector Monte Carlo simulation is based on GEANT4: S. Agostinelli *et al.*, Nucl. Instrum. Methods Phys. Res., Sect. A **506**, 250 (2003); Simulated events are generated with Jetset 7.4: T. Sjöstrand and M. Bengtsson, Comput. Phys. Commun. **43**, 367 (1987).
- [11] J.E. Gaiser, Ph.D. thesis, Stanford University [SLAC Report No. SLAC-R-255, 1982].
- [12] C. Amsler *et al.* (Particle Data Group), Phys. Lett. B **667**, 1 (2008).
- [13] W. Kwong, P.B. Mackenzie, R. Rosenfeld, and J.L. Rosner, Phys. Rev. D **37**, 3210 (1988); C.S. Kim, T. Lee, and G.L. Wang, Phys. Lett. B **606**, 323 (2005); J.P. Lansberg and T.N. Pham, Phys. Rev. D **75**, 017501 (2007).
- [14] B.A. Kniehl *et al.*, Phys. Rev. Lett. **92**, 242001 (2004); S. Recksiegel and Y. Sumino, Phys. Lett. B **578**, 369 (2004).